Cancer Therapy: Preclinical

Clinical Cancer Research

Preclinical Activity of the Liposomal Cisplatin Lipoplatin in Ovarian Cancer

Naike Casagrande[1], Marta Celegato[1], Cinzia Borghese[1], Maurizio Mongiat[1], Alfonso Colombatti[1,2], and Donatella Aldinucci[1]

Abstract

Purpose: Cisplatin and its platinum derivatives are first-line chemotherapeutic agents in the treatment of ovarian cancer; however, treatment is associated with tumor resistance and significant toxicity. Here we investigated the antitumoral activity of lipoplatin, one of the most promising liposomal platinum drug formulations under clinical investigation.

Experimental Design: *In vitro* effects of lipoplatin were tested on a panel of ovarian cancer cell lines, sensitive and resistant to cisplatin, using both two-dimensional (2D) and 3D cell models. We evaluated *in vivo* the lipoplatin anticancer activity using tumor xenografts.

Results: Lipoplatin exhibited a potent antitumoral activity in all ovarian cancer cell lines tested, induced apoptosis, and activated caspase-9, -8, and -3, downregulating Bcl-2 and upregulating Bax. Lipoplatin inhibited thioredoxin reductase enzymatic activity and increased reactive oxygen species accumulation and reduced EGF receptor (EGFR) expression and inhibited cell invasion. Lipoplatin demonstrated a synergistic effect when used in combination with doxorubicin, widely used in relapsed ovarian cancer treatment, and with the albumin-bound paclitaxel, Abraxane. Lipoplatin decreased both ALDH and CD133 expression, markers of ovarian cancer stem cells. Multicellular aggregates/spheroids are present in ascites of patients and most contribute to the spreading to secondary sites. Lipoplatin decreased spheroids growth, vitality, and cell migration out of preformed spheroids. Finally, lipoplatin inhibited more than 90% tumor xenograft growth with minimal systemic toxicity, and after the treatment suspension, no tumor progression was observed.

Conclusion: These preclinical data suggest that lipoplatin has potential for clinical assessment in aggressive cisplatin-resistant patients with ovarian cancer. *Clin Cancer Res; 20(21); 5496–506. ©2014 AACR.*

Introduction

Ovarian cancer is the fifth leading cause of cancer-related death in women in developed countries and has one of the highest ratios of incidence to death (1). The standard postoperative chemotherapy for epithelial ovarian cancer is a combination therapy including cisplatin and taxanes. Most patients are responsive to chemotherapy at first; however, toxicity and acquired resistance to cisplatin have proven challenging and represent the major obstacle to improve the prognosis of patients with ovarian cancer (1). Cisplatin resistance is due to a broad panel of molecular and functional alterations, including the reduced intracellular accumulation through the copper transporter 1 (Ctr1) and the increased efflux through the cell membrane (2). Thus, the development of new cisplatin formulations or the encapsulation into liposomes to overcome both resistance and toxicity remains a high priority (3).

While various formulations of cisplatin encapsulated into liposomes demonstrated a good anticancer activity *in vitro*, the results obtained *in vivo* were often disappointing (3). One example is SPI-77, which did not produce significant clinical response rates in several phase II studies of patients with inoperable head and neck cancer, advanced non–small cell lung cancer (NSCLC; ref. 4), and also in ovarian cancer (5). The lack of therapeutic efficacy was likely due to slow and inefficient release of platinum from SPI-77.

Lipoplatin is one of the most promising liposomal platinum drug formulations under clinical investigation (3, 4, 6). It has shown similar efficacy as cisplatin in pancreatic, head and neck cancer, NSCLC, and HER-2/neu–negative metastatic breast cancer with a major benefit of a strongly reduced toxicity (6, 7).

[1]Experimental Oncology 2, CRO Aviano National Cancer Institute, Aviano, Italy. [2]Department of Medical and Biological Science Technology and MATI (Microgravity Ageing Training Immobility) Excellence Center, University of Udine, Udine, Italy.

Note: Supplementary data for this article are available at Clinical Cancer Research Online (http://clincancerres.aacrjournals.org/).

Corresponding Author: Donatella Aldinucci, Experimental Oncology 2, CRO Aviano National Cancer Institute, via F. Gallini 2, Aviano I-33081, Italy. Phone: +39-0434-659234; Fax: +39-0434-659428; E-mail: daldinucci@cro.it

doi: 10.1158/1078-0432.CCR-14-0713

©2014 American Association for Cancer Research.

Downloaded from http://aacrjournals.org/clincancerres/article-pdf/20/21/5496/2022082/5496.pdf by guest on 21 July 2024

Translational Relevance

At present, the standard treatment for ovarian cancer involves tumor debulking with platinum-based chemotherapy. The response to this regimen is at least 70% of patients; however, 60% to 80% of the first responders relapse within 18 months with a platinum-resistant disease. Lipoplatin is one of the most promising liposomal platinum drug formulations under clinical investigation. Our preclinical data demonstrated that lipoplatin was active in a panel of ovarian cancer cell lines, including cisplatin-resistant cells. We have shown that lipoplatin induced apoptosis and ROS production, reduced spheroid growth and migration, and reduced cancer stem cell (CSC) number. Lipoplatin inhibited xenograft tumor growth to more than 90% and with low toxicity, whereas the effective dose of cisplatin was too toxic for the animals. Lipoplatin showed a synergistic activity with doxorubicin and Abraxane. This preclinical data provide the rationale for the clinical assessment of lipoplatin in aggressive cisplatin-resistant patients with ovarian cancer.

Lipoplatin nanoparticles fuse with the cell membrane or are rapidly taken up by cancer cells by their avidity for nutrients, as shown with fluorescent nanoparticles, and lipoplatin disguises as a nutrient with its lipid shell (6). Thus, the toxic payload enters the cytoplasm bypassing active import, explaining the efficacy of lipoplatin against platinum-resistant tumors (6). Accordingly, we demonstrated that lipoplatin is active both *in vitro* and *in vivo* against cisplatin-resistant cervical cancer cells (8). Lipoplatin has an enhanced half-life circulation time in body fluids and tissues and can extravasate through the leaky tumor vasculature reaching concentrations 10- to 200-fold higher in the tumor or metastases than in the adjacent normal tissues. During their extravasation into primary and metastatic tumor tissue shown in human studies (9), lipoplatin nanoparticles attack not only the epithelial cancer cells linked to the property of classic cisplatin chemotherapy but also the endothelial cells of tumor vasculature because of their lipid nature; thus, lipoplatin is acting as a chemotherapeutic and antiangiogenic drug (10). The greater the vascularization of the tumor, the greater the concentration of lipoplatin in the tumor or metastasis (9).

Given the properties of lipoplatin to overcome cisplatin resistance and to induce low toxicity (6, 8), this drug could represent a good alternative to cisplatin. The aim of our study was to analyze the efficacy of lipoplatin in the ovarian cancer setting. Although many drugs show promising results *in vitro*, the success rate of anticancer therapies translating from *in vitro* culture systems into the clinic is about 5%, suggesting the use of multiple techniques during the preclinical evaluation of new anticancer agents. Thus, using the *in vitro* traditional 2-dimensional (2D) model, the *in vitro* 3D cell culture, which seems to better reflect the histologic, biologic, and molecular features of primary tumors (11), and the *in vivo* tumor xenograft tumor, we demonstrated that lipoplatin was active against cisplatin-resistant cells in both monolayer cultures (2D model) and spheroids (3D model), it synergized with doxorubicin and Abraxane and proved to be very effective *in vivo*.

Materials and Methods

Drugs

Lipoplatin, the liposomal formulation of cisplatin labeled with fluorescein isothiocyanate (FITC), and lipoplatin (lipoplatin-FITC; ref. 6) were generously provided by Regulon Inc. Cisplatin was purchased from Mayne Pharma, carboplatin from Teva (Pharma Italia, S.r.l), Abraxane (Nab-Paclitaxel) from Celgene, doxorubicin from Pfizer, docetaxel from Hospira, and paclitaxel from Actavis. Drugs were dissolved in medium at the indicated concentrations immediately before use.

Cell lines and culture conditions

Human ovarian epithelial carcinoma–derived cancer cell lines MDAH 2774 (ATCC CRL-10303), OVCAR3 (ATCC HTB-161), SKOV3 (ATCC HTB-77), TOV21G (ATCC CRL-11730) were purchased from the ATCC; A2780 and its cisplatin-resistant clone A2780cis from Sigma, Inc. OVCAR5 (NIH) cells were provided by Dr. Baldassarre (CRO, Aviano, Italy). Cell lines were further authenticated for their origin by BMR Genomics on January 2012 according to Cell ID System (Promega) protocol and using Genemapper ID Ver 3.2.1 to identify DNA short tandem repeat profiles. Histology origins included ovarian carcinoma from an untreated patient (A2780 and its cisplatin-resistant clone A2780cis), clear cell carcinoma (TOV21G), endometrioid carcinoma (MDAH), and malignant cells derived from the ascites (OVCAR3, OVCAR5, and SKOV3). Cells were cultured in RPMI (Sigma-Aldrich) supplemented with 10% heat-inactivated FBS (Sigma), 0.2 mg/mL penicillin/streptomycin (Sigma), and 0.1% (w/v) L-glutamine (Sigma) at 37°C in a 5% CO_2 fully humidified atmosphere.

Cytotoxicity assay

Cells (4.0×10^3) were cultured in a 96-well, flat-bottom plate and was treated with increasing concentrations of lipoplatin (2.5–100 μmol/L), cisplatin (2.5–100 μmol/L), or carboplatin (2.5–200 μmol/L) at 37°C for 72 hours. Triplicate cultures were established for each treatment. Cytotoxicity was measured by using the MTT assay. The half maximal inhibitory concentration (IC_{50}) value was calculated using the CalcuSyn software (Biosoft; ref. 12).

Experimental design for drug combinations and Chou–Talalay analysis for synergy

First, we determined the IC_{50} values for doxorubicin, Abraxane, docetaxel, and paclitaxel for OVCAR5 and SKOV3. Then, 4.0×10^3 cells were incubated with each drug alone or in combination for 72 hours, and cytotoxicity was evaluated by MTT assay. The combined drug effects

Downloaded from http://aacrjournals.org/clincancerres/article-pdf/20/21/5496/2022082/5496.pdf by guest on 21 July 2024

were calculated using the diagonal constant ratio combination (12). Synergy was determined calculating the combination index (CI) using CalcuSyn software. A CI value of 1 indicates an additive effect between 2 drugs. CI values less than 1 indicate synergy; the lower the value, the stronger the synergy. On the contrary, CI values more than 1 indicate antagonism.

Flow cytometry

Cells (5.0×10^4) were incubated for 72 hours on 6-well plates in complete medium in the presence of (30 μmol/L) lipoplatin. Annexin V binding [Becton Dickinson (BD) Pharmingen], DNA fragmentation (Apo-Direct kit, BD), changes in mitochondrial membrane potential (MitoTracker Red CMXRos, Invitrogen), cytochrome *c* (cyt *c*) release (BD; see Supplementary Materials and Methods), caspase-3, -8, and -9 activation (Chemicon International), mitochondrial reactive oxygen species (ROS; MitoSox reagent working solution, Molecular Probes, Invitrogen), Bcl-2 (DAKO Cytomation), Bcl-xL (Cell Signalling), Bax (BD), anti-EGFR monoclonal antibody (mAb) 528 (Santa Cruz Biotechnology Inc.), and CD133 (AC133, Miltenyi Biotec) were evaluated as previously described (8, 13). Cell cycle was evaluated by propidium iodide (PI) staining. Aldehyde dehydrogenase (ALDH) activity was evaluated using Aldeflour reagent–based method (Stem Cell Technologies). Briefly, cells (2×10^5/mL) were incubated for 40 minutes at 37°C with Aldeflour reagent with and without the ALDH inhibitor (DEAB). Viable antibody-labeled cells were identified according to their forward and right angle scattering, electronically gated and analyzed on a FACSCalibur flow cytometer (BD), using CellQuest Software (BD).

Thioredoxin reductase enzymatic activity assay

Cells (7.5×10^4) were treated with lipoplatin (20–30 μmol/L) for 72 hours. Thioredoxin reductase (TrxR) activity was assessed using the Thioredoxin Reductase Assay Kit (Sigma-Aldrich; ref. 13).

Invasion assay

Invasion was assessed by the FATIMA assay (8). After drug treatment (72 hours with 10 μmol/L lipoplatin), cells (1.0×10^5 cells/insert) tagged with the lipophilic dye Fast DiI (Molecular Probes) were seeded in 150 μL of serum-free medium in the upper side of collagen type I–coated Boyden chamber inserts. Complete medium with 20% FCS was used as chemoattractant. Invasion was monitored using a computer-interfaced GeniusPlus microplate reader (Tecan), and the percentage of transmigrated cells was determined by FATIMA software.

3D multicellular spheroid formation assays, growth, and migration

To obtain spheroids, 48-well plates were coated twice with 20 mg/mL of poly-HEMA [poly(2-hydroxyethyl methacrylate); Sigma; ref. 14] in 95% ethanol and washed once with PBS before cell seeding. Spheroids were generated by plating 5×10^4 SKOV3 cells in complete medium. To evaluate the effect of lipoplatin on spheroid formation, cells were cultured in poly-HEMA–coated 48 wells in the presence of the drug (10, 25, or 50 μmol/L). After 72 hours, spheroids were photographed, harvested, and dissociated into single-cell suspensions by trypsinization, then the extent of apoptosis (Annexin V/PI staining) was determined (15). Alternatively, lipoplatin or cisplatin activity was evaluated on preformed single spheroids as described (14). Briefly, 1.0×10^4 SKOV3 cells were dispensed into poly-HEMA–coated round-bottom, 96-well plates. After 4 days, spheroids were treated with increasing concentrations of lipoplatin (25, 50 μmol/L). Spheroid size was measured up to 15 days after lipoplatin treatment initiation. A 50% medium replacement was performed on days 3, 7, 10, and 15. Responses were evaluated by the measurement of spheroid size at regular intervals (16) using an inverted microscope (Eclipse TS/100, Nikon) with photomicrographic systems DS Camera Control Unit DS-L2. Spheroid volumes were calculated using the formula: $(\text{width}^2 \times \text{length} \times 3.14)/6$ (17). To assess cell viability, spheroids were incubated for 30 minutes with 2 μg/mL PI and then observed under laser fluorescence microscope (DMI 600013, Leica; original magnification, 4×). Single spheroids were incubated with 1:50 lipoplatin-FITC (6). Spheroid images were acquired using the confocal microscope (Leica DM IRE2) to trace the penetration of lipoplatin-FITC. Migration/dissemination (14) assay was performed in 96-well plates precoated with 10 μg/mL collagenase I (Sigma-Aldrich) and blocked with BSA (1 mg/mL) for 2 hours. Preformed spheroids were layered (3–5 spheroids per well) in the 96-well plates in the absence or presence of lipoplatin (25, 50 μmol/L). Image analysis software was used to calculate the spheroid size. The extent of migration was determined using Adobe Photoshop by outlining the entire area of the dispersed cells (14). The fold change in area was calculated dividing the pixel area of the spheroid at 24 and 48 hours by the pixel area at time 0.

Tumor xenograft experiments

All the *in vivo* studies were approved by the Institutional Ethics Committee. Six-week-old female athymic *nu/nu* (nude) mice were purchased from Charles River, and 2.7×10^6 OVCAR5 cells suspended in 0.1 mL of Matrigel 1:3) in PBS) were inoculated in the right flank of each mouse. When tumors reached about 44 mm^3 in volume, mice were divided randomly into 2 groups of 8 mice each and were treated 3 times per week with intraperitoneal injection of 20 mg/kg lipoplatin or drug-free vehicle. Tumor size was measured over time using a caliper, and volumes were calculated according to the standard formula: $(\text{width}^2 \times \text{length} \times 3.14)/6$. At day 39, the treatment was suspended for 14 days. When control tumors had reached a volume of about 1,000 mm^3, mice were sacrificed. The mouse organs were excised and fixed in formalin for tissue toxicity analyses. Sections were cut and counterstained with hematoxylin and eosin according to standard procedures.

Downloaded from http://aacrjournals.org/clincancerres/article-pdf/20/21/5496/2022082/5496.pdf by guest on 21 July 2024

Software and statistical analysis of data

Values are presented as the mean with the standard error of not less than 3 measurements (unless otherwise stated; mean ± SEM). To estimate the equal sample size for the mouse study groups, the experiment was designed to be able to detect a 0.60 difference with 0.90 power and an α error of 0.05. Statistical analysis was performed using GraphPad Prism 6 Software (GraphPad). The statistical significance of differences was determined by the Student *t* test for comparison between 2 groups. ANOVA was used to evaluate the correlation of data among 3 or more groups; consecutive multiple comparison analysis was performed using Dunnett or Tukey tests. Differences were considered statistically significant at $P < 0.05$.

Results

Lipoplatin inhibited proliferation and induced apoptosis in cisplatin-sensitive and -resistant ovarian cancer cell lines

First, we evaluated the *in vitro* cytotoxic effects of lipoplatin, cisplatin, and carboplatin (Fig. 1A) on a panel of ovarian cancer cell lines with different sensitivities to cisplatin. Treatment with lipoplatin induced a dose-dependent inhibition of cell proliferation with IC_{50} value ranging from 14.6 in MDAH to 32.1 μmol/L in OVCAR3 cells (Fig. 1A, top). The IC_{50} for lipoplatin was higher (about 4-fold) than that of cisplatin (Fig. 1A, middle) in all cell lines tested excluding OVCAR5 that had a similar sensitivity to both drugs (Fig. 1A). On the contrary, A2780 (cisplatin, IC_{50} = 1.46 μmol/L) and its cisplatin-resistant clone A2780cis (cisplatin, IC_{50} = 10.3 μmol/L) showed a comparable sensitivity to lipoplatin (IC_{50} = 17.8 and 17.7 μmol/L, respectively; Fig. 1A, top). Thus, lipoplatin exhibited a similar cytotoxic effect in cell lines with different histologic origins and with a wide range of sensitivity to cisplatin, including cell lines considered cisplatin-resistant (18).

The sensitivity of ovarian cancer cell lines to carboplatin was very similar to that of cisplatin, excluding TOV21G cells (Fig. 1A, bottom). A2780 cells were more sensitive to carboplatin than A2780cis that showed the highest IC_{50} together with OVCAR5 and TOV21G cells.

Next, to measure lipoplatin efficacy to induce cell-cycle modifications and apoptosis, we used OVCAR5 (the least sensitive cell line to cisplatin) and SKOV3 cells [intrinsic cisplatin-resistant (ref. 18) and forming spheroids]. Treatment for 24 hours with lipoplatin (30 μmol/L) induced an increase in the S- and G_2–M phases in OVCAR5 cells and a block in G_2–M phase in SKOV3 cells (data not shown). Lipoplatin induced apoptosis in a dose-dependent manner, as evaluated by the Annexin V/PI staining (Fig. 1B), the activation of caspase-9, -8, and -3 (Fig. 1C), and DNA fragmentation (Fig. 1D, left). In analogy with cisplatin (19), lipoplatin decreased the mitochondrial membrane potential (Fig. 1D, middle) and induced cyt *c* release (Fig. 1D, right). Lipoplatin increased the proapototic molecule Bax, decreased the antiapoptotic Bcl-2, and only slightly decreased Bcl-xL expression (Fig. 1E). Lipoplatin increased ROS production (Fig. 2A and B) and reduced the enzymatic activity of TrxR (Fig. 2C), a selenoenzyme essential to maintain the cellular redox status and to protect against oxidative damage due to ROS accumulation (20), in a dose-dependent manner in both cell lines.

In addition, we evaluated lipoplatin activity in A2780 and its cisplatin-resistant clone A2780cis. Even if A2780 and A2780cis had the same IC_{50} for lipoplatin, the drug induced significant apoptosis (Supplementary Fig. S1A–S1C) and ROS formation (Supplementary Fig. S1D and S1E) only in A2780 cells. On the contrary, while lipoplatin was able to stop cell growth, it only slightly increased Annexin V staining and ROS formation in A2780cis (Supplementary Fig. S1). A2780cis and OVCAR5 cells had similar IC_{50} values; however, cisplatin induced apoptosis and ROS formation only in A2780 and A2780cis, but not in OVCAR5 cells (Supplementary Fig. S2).

Taken together, our results suggest that different mechanisms of resistance are involved in A2780cis, obtained by *in vitro* selection with cisplatin, and OVCAR5 cells, derived from ascitic fluid of a patient with progressive ovarian adenocarcinoma without prior cytotoxic treatment.

Lipoplatin synergized with doxorubicin and Abraxane

The standard treatment of patients with advanced ovarian cancer is cytoreductive surgery followed by combination chemotherapy with taxanes or doxorubicin and platinating agents (21, 22). We also evaluated whether the combination of lipoplatin with doxorubicin (Table 1) or with either of the 3 different taxanes, docetaxel, paclitaxel, and the albumin-stabilized paclitaxel Abraxane (refs. 23, 24; Table 1), was more effective than each agent used separately. OVCAR5 cells were less sensitive (IC_{50} = 0.87 μmol/L) to doxorubicin than SKOV3 cells (IC_{50} = 0.13 μmol/L; Table 1); however, lipoplatin and doxorubicin synergized in both cell lines (CI < 1.0; Table 1). While the combination of lipoplatin with paclitaxel or docetaxel resulted in additive effects in OVCAR5 and in low synergy in SKOV3 cells, Abraxane showed clear synergistic activity in both cell lines (CI < 1; Table 1).

In OVCAR5, we observed a high synergistic activity of cisplatin with doxorubicin and Abraxane, but not with paclitaxel and docetaxel. In SKOV3, cisplatin strongly synergized with all the 4 drugs and especially with Abraxane (Supplementary Table S1). Finally, the combination of carboplatin with doxorubicin exerted very low synergistic (OVCAR5) or additive (SKOV3) effects. In SKOV3 cells, all the 3 taxanes exerted a significant synergistic activity, whereas in OVCAR5, only paclitaxel displayed synergy (Supplementary Table S2).

Lipoplatin inhibited invasion and downmodulated EGFR expression

To exclude that a lower migration rate could be attributable to a decreased cell proliferation, cells were cultured for

Downloaded from http://aacrjournals.org/clincancerres/article-pdf/20/21/5496/2022082/5496.pdf by guest on 21 July 2024

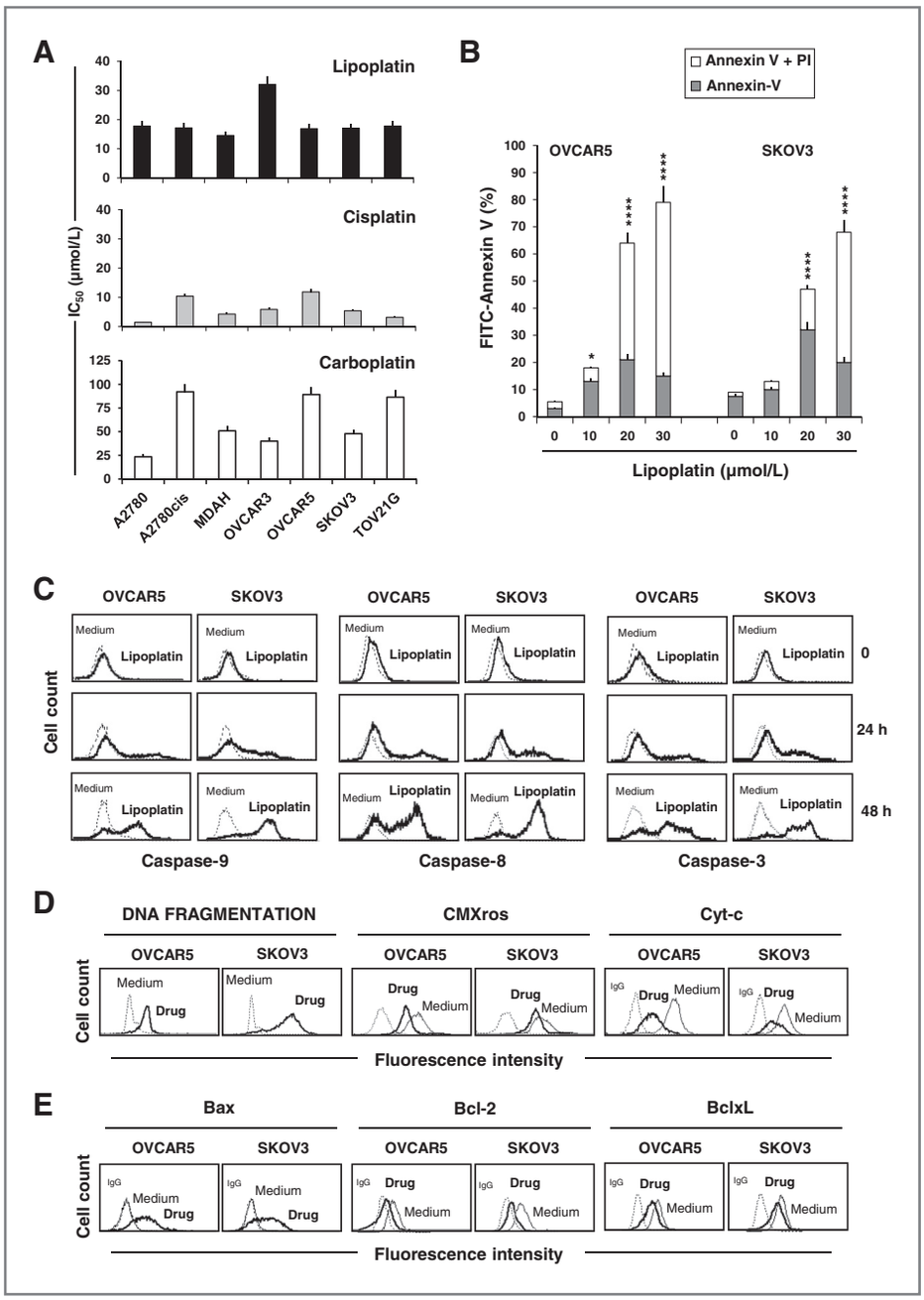

Figure 1. Lipoplatin induces mitochondria-mediated apoptosis and modulates Bax, Bcl-2, and Bcl-xL expression. A, cells were cultured for 72 hours in the presence of increasing concentrations of lipoplatin, cisplatin, or carboplatin. IC_{50} was obtained using the CalcuSyn software. Values in the bar graph represent the mean $IC_{50} \pm$ SEM of different experiments. B, FACS analysis of cells after 72-hour incubation with different concentrations of lipoplatin and double stained with Annexin V/FITC and PI. Values in the bar graph represent the mean ± SEM of 3 different experiments. *, $P < 0.05$; ****, $P < 0.0001$ drug versus medium. C, analysis of caspase-9, -8, and -3 activation after incubating cells with lipoplatin (30 μmol/L) for 24 and 48 hours. Cells were harvested, washed, and resuspended in complete medium supplemented with FLICA for 1 hour at 37°C, then washed again and analyzed by flow cytometry. Dotted lines indicate background fluorescence of cells. The *x*- and *y*-axes indicate the logarithms of the relative fluorescence intensity and relative cell number, respectively. FACS histograms are representative of 1 of 3 different experiments. D, DNA fragmentation (Apo-Direct), mitochondrial membrane permeabilization (CMXRos), and cyt *c* release were assessed by flow cytometry after treatment for 72 hours with lipoplatin (30 μmol/L). E, analysis of Bax, Bcl-2, and Bcl-xL expression. Cells were incubated with lipoplatin (30 μmol/L) for 72 hours and then Bax, Bcl-2, and Bcl-xL expression was assessed by flow cytometry.

72 hours in the presence of less drug (10 μmol/L) and at low serum concentration. Then, we evaluated cell invasion through a type I collagen–coated Boyden chamber. Already at 5 hours, lipoplatin decreased invasion of about 45% and 51% in OVCAR5 and SKOV3 cells, respectively (Fig. 3A), and this level of inhibition was maintained at 24 hours. EGFR is usually overexpressed in ovarian carcinoma, and its activation is related not only to survival but also to invasion and metastasis (25). Both OVCAR5 and SKOV3 had similar invasive properties (Fig. 3A) and expressed high levels of EGFR (Fig. 3B and C). Lipoplatin downregulated in a dose-dependent manner EGFR expression (Fig. 3B and C).

Lipoplatin reduced ALDH$^+$ and CD133$^+$ cells and inhibited both growth and migration of cells from preformed spheroids

Together with the ability to form spheroids (26), the enzymatic activity of ALDH and CD133 expression (27) are considered markers of ovarian CSCs and of drug resistance. OVCAR5 expressed higher amounts (~2-fold) of ALDH$^+$ cells than SKOV3 (Fig. 4A). CD133 expression was

Downloaded from http://aacrjournals.org/clincancerres/article-pdf/20/21/5496/2022082/5496.pdf by guest on 21 July 2024

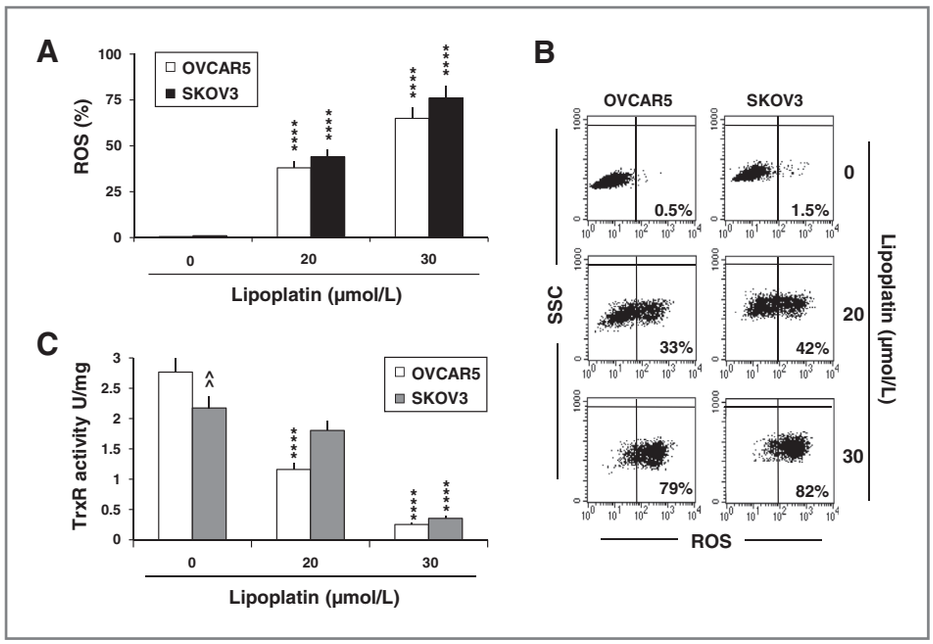

Figure 2. Lipoplatin induces ROS accumulation and inhibits TrxR activity. A, ROS production: cells were treated with lipoplatin for 72 hours, and the bar graphs represent the percentage of ROS as the mean ± SEM of 3 different experiments. B, representative FACS dot plots of 1 of 3 independent experiments showing ROS generation. C, TrxR enzymatic activity: values in the bar graph represent the mean ± SEM of 3 different experiments ****, $P < 0.0001$ drug versus medium; ^^, $P < 0.0001$ OVCAR5 versus SKOV3.

similar (~5%) in both OVCAR5 and SKOV3 cells. Treatment with lipoplatin decreased in a dose-dependent manner the ALDH enzymatic activity (Fig. 4A and B) and CD133 expression (Fig. 4C and D) in both cell lines.

Spheroids represent a 3D *in vitro* system that more closely resembles the *in vivo* tumor microenvironment and a more efficacious first-line approach to study drug activity and the invasive phenotype (11, 28). In agreement with the study by Lee and colleagues (11), OVCAR3 and MDAH could spontaneously form large loose aggregates or spheroids; OVCAR5, TOV21G, A2780, and A2780cis formed small aggregates (data not shown); and the SKOV3 cell line formed large dense aggregates (LDA)/spheroids. On the basis of their ability to form LDAs/spheroids, we used SKOV3 cells to quantify lipoplatin activity also in 3D conditions.

Spheroids obtained by SKOV3 cells increased their volume in a time-dependent manner, reaching a 6-fold increase after 15 days of cultivation (Fig. 5A and B). Lipoplatin, like cisplatin (Supplementary Fig. S3A), inhibited the spheroid growth (Fig. 5A and B) in a dose-dependent manner. Lipoplatin increased the PI-positive dead cells (Fig. 5C). Consistently, we found that lipoplatin-FITC deeply penetrated into spheroids (Fig. 5D). Lipoplatin decreased

Table 1. CI values for OVCAR5 and SKOV3 cell lines treated with lipoplatin and doxorubicin, Abraxane, docetaxel, or paclitaxel

Cell lines	Lipoplatin, μmol/L	Doxorubicin, μmol/L	CI	Abraxane, ng/mL	CI	Docetaxel, nmol/L	CI	Paclitaxel, ng/mL	CI
OVCAR5	4.23	0.21	0.617	8.42	0.687	4.51	0.947	6.32	1.282
	8.46	0.43	0.839	16.84	0.415	9.02	1.105	12.64	0.623
	16.93[a]	0.87[a]	0.488	33.68[a]	0.325	18.04[a]	0.683	25.27[a]	0.752
	33.86	1.73	0.718	67.36	0.539	36.08	0.729	50.54	0.808
	67.72	3.46	1.222	134.72	1.220	72.16	1.260	101.08	1.119
SKOV3	4.26	0.03	1.390	11.76	0.381	10.23	0.524	34.11	0.682
	8.53	0.06	0.877	23.52	0.536	20.45	0.728	68.23	0.586
	17.06[a]	0.13[a]	0.385	47.05[a]	0.507	40.90	0.696	136.45[a]	0.706
	34.12	0.26	0.586	94.10	0.723	81.80	0.636	272.90	0.617
	68.24	0.52	1.420	188.20	1.380	163.60	1.190	545.80	0.950

NOTE: Cells were incubated with each drug alone or in combination for 72 hours, and then cell viability was determined by the MTT assay and the CI calculated using the CalcuSyn software.

[a]The IC_{50} for each drug.

Downloaded from http://aacrjournals.org/clincancerres/article-pdf/20/21/5496/2022082/5496.pdf by guest on 21 July 2024

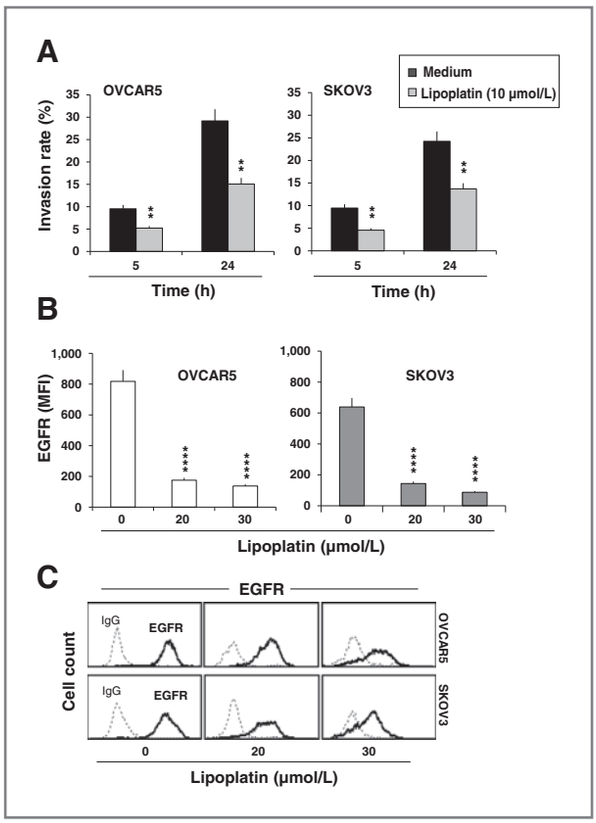

Figure 3. Lipoplatin inhibits invasion and decreases EGFR expression. A, invasion of ovarian cancer cells through a collagen type I–coated Boyden chamber after treatment for 72 hours with 10 μmol/L lipoplatin. Values in the bar graph represent the mean ± SEM of 3 different experiments. **, $P < 0.01$, drug versus medium. B, EGFR surface expression: cells were treated for 72 hours with lipoplatin and analyzed by flow cytometry using the anti-EGFR mAb 528. Values in the bar graph represent the mean ± SEM of 3 different experiments. ****, $P < 0.0001$ drug versus medium. MFI, mean fluorescence intensity. C, representative FACS histograms of 1 of 3 independent experiments showing the decrease of EGFR expression after drug treatment.

the capability of SKOV3 cells to migrate/disseminate out of the spheroids with a 50% reduction of the area covered by migrating cells (Fig. 5E and F).

Lipoplatin inhibited the growth of ovarian cancer xenografts

We also analyzed the anticancer activity of lipoplatin *in vivo*. For this purpose, OVCAR5 cells (2.7×10^6) were injected into the right flank of 6-week-old female athymic nude mice and, once tumors reached a volume of about 44 mm^3, the mice were treated intraperitoneally 3 times a week with vehicle alone or with vehicle containing lipoplatin (20 mg/kg). Significant tumor growth inhibition by lipoplatin was apparent after 17 days of treatment (Fig. 5G). At day 41, the control tumors grew to a mean 417.2 ± 5 mm^3 in size, whereas lipoplatin showed an 82% inhibitory effect, as the treated tumors reached a mere size of 73.12 ± 8 mm^3 (**, $P < 0.01$; Fig. 5G). The treatment was suspended (Fig. 5F, dashed lines) and mice were followed for 14 more days. Tumors of untreated mice continued to grow (Fig. 5G) and after 14 days doubled their size and reached a volume of 969.74 ± 8 mm^3, whereas tumors of lipoplatin-treated mice were inhibited by more than 90%. While treatment with the same concentration of cisplatin was lethally toxic for mice, there was no histologically detectable cytotoxicity involving the animals' heart, spleen, liver, and kidney in mice treated with lipoplatin (data not shown). A sublethal dose of cisplatin (6 mg/kg; ref. 29) led to a significant decrease of tumor growth (Supplementary Fig. S3B) but was still severely toxic for the animals (Supplementary Fig. S3C). Mice experienced a significant weight loss (~50% of control), 2 of 5 mice died (at day 22) during the treatments and 2 had to be euthanized (at day 28) to avoid further suffering, before the end of the experiment (at day 42). An even lower dose of cisplatin (3 mg/kg) was not toxic for the animals and did not affect tumor growth (Supplementary Fig. S3B and S3C).

Discussion

Cisplatin is very effective for the treatment of ovarian cancers; however, its severe toxicity and the emergence of primary or acquired resistance limit its efficacy. In this study, we investigated the biologic activity and molecular mechanisms of action of a new formulation of cisplatin, lipoplatin, the most clinically active formulation of liposomal-encapsulated cisplatin to date (3, 6).

Lipoplatin affected cell proliferation, exhibiting a similar cytotoxic effect in ovarian cancer cell lines of different histologic origins and with a wide range of cisplatin sensitivity, including cisplatin-resistant cell lines. Lipoplatin exerted its cytotoxic effect by inducing apoptosis, as previously demonstrated in cervical cancer (8), determined mitochondrial membrane depolarization, cyt *c* release, and the activation of both caspase-9 and -3. Consistent with recent studies demonstrating that another formulation of liposomal cisplatin induced the extrinsic apoptotic pathway in the cisplatin-resistant A2780cis cells (30, 31), we found that lipoplatin also activated caspase-8, indicating that the activity of this drug was exerted through the mitochondrial intrinsic and the extrinsic apoptotic pathways. Lipoplatin significantly affected the expression of 2 regulators of the mitochondrial apoptotic pathway: it decreased the prosurvival protein Bcl-2 and increased the proapoptotic Bax protein (32, 33).

The IC_{50} for lipoplatin was higher than that for cisplatin but similar in OVCAR5- and in A2780cis-resistant cells. However, it should be considered that other liposomal cisplatin showed similar IC_{50} in A2780 and A2780cis cells (30, 31). Moreover, we found that lipoplatin but not cisplatin, used at the same concentration, induced apoptosis and ROS generation in OVCAR5 but not in A2780cis, thus suggesting that distinct liposomal formulations could result in different cytotoxic activities and that different mechanisms of resistance to cisplatin are involved between OVCAR5 and A2780cis.

The antioxidant TrxR system maintains the intracellular redox state and defends cells against oxidative damage due

Downloaded from http://aacrjournals.org/clincancerres/article-pdf/20/21/5496/2022082/5496.pdf by guest on 21 July 2024

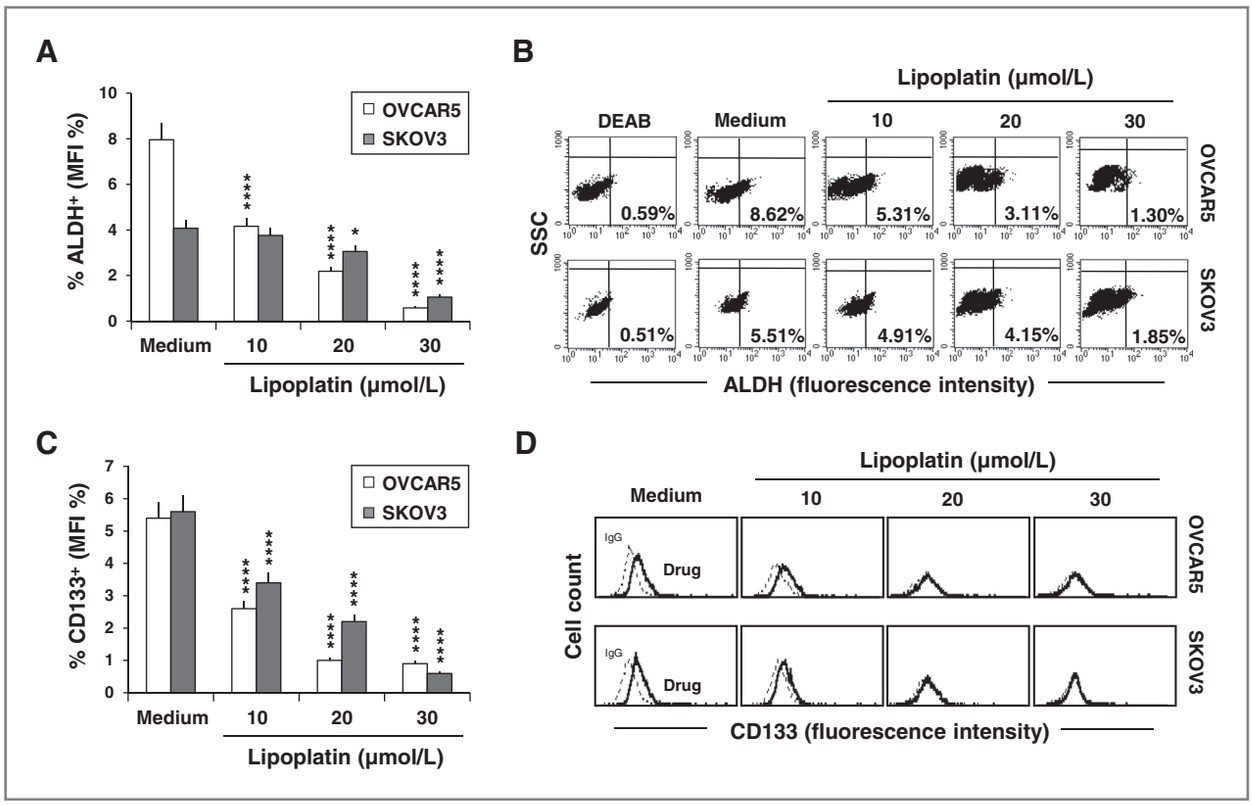

Figure 4. Lipoplatin reduces CD133$^+$ and ALDH$^+$ cells. Cells were treated with different concentrations of lipoplatin (10, 20, 30 μmol/L). A, quantification of ALDH as percentage of positive cells. Values in the bar graph represent the mean ± SEM of 3 different experiments. The ALDH inhibitor diethylaminobenzaldehyde (DEAB) was used as negative control. B, representative FACS dot plots of 1 of 3 independent experiments showing ALDH quantification (% of positive cells) after lipoplatin treatment. C, quantification of CD133 as percentage of positive cells. Values in the bar graph represent the mean ± SEM of 3 different experiments. D, representative FACS histograms of 1 of 3 independent experiments showing CD133 expression after lipoplatin treatment. *, $P < 0.05$; ****, $P < 0.0001$ drug versus medium. MFI, mean fluorescence intensity.

to ROS overproduction, leading to the formation of proapoptotic molecules (34). TrxR is upregulated in many malignant tumors (34, 35) and plays a central role against drug-induced oxidative stress, suggesting that this enzyme could become a suitable target for anticancer therapy. Lipoplatin, in analogy with cisplatin (36), inhibited TrxR enzymatic activity and induced the generation of large amounts of mitochondrial superoxide.

Lipoplatin, and especially cisplatin, demonstrated a synergistic effect with doxorubicin, a chemotherapeutic drug widely used in relapsed ovarian cancer treatment (21), and with the albumin-bound paclitaxel, Abraxane. Abraxane was the only taxane of the 3 tested capable of synergizing with lipoplatin, as docetaxel and paclitaxel essentially exerted additive effects. Abraxane was more active than docetaxel and paclitaxel also in combination with cisplatin, but not with carboplatin. It is of note that Abraxane is used in phase II clinical trials in patients with recurrent platinum-resistant primary epithelial ovarian or primary peritoneal carcinoma, as it displays reduced toxicity with respect to paclitaxel (37).

EGFR overexpression and activation is related to ovarian cancer progression and increased migration (38). However, small-molecule inhibitors of EGFR tyrosine kinase activity, such as erlotinib, exhibited very limited activity as single agents in patients with recurrent or persistent ovarian cancer (39). Recently, we demonstrated that lipoplatin decreased EGFR expression and cell migration in cervical cancer cells (8). Similarly, we found here that lipoplatin downregulated EGFR expression and decreased cell migration, thus suggesting that it could not only exert direct cytotoxic effects on ovarian cancer cells but also decrease tumor invasion and/or proliferation induced by EGFR activation. Because ovarian carcinoma has a very poor rate of survival and is characterized by the presence of diffuse peritoneal metastases (40), this significant activity of lipoplatin could also be useful in highly aggressive, poor-prognosis subgroup of high-grade malignant ovarian cancer characterized by the co-expression of ALDH/EGFR (41).

Together with the enzymatic activity of ALDH, the expression of CD133 is considered a marker of ovarian CSCs and is associated with drug resistance (27, 42, 43). Accordingly, lipoplatin reduced the percentage of ALDH$^+$ and CD133$^+$ cells, suggesting that lipoplatin could eliminate ovarian CSCs that are more chemo- and radioresistant than the

Downloaded from http://aacrjournals.org/clincancerres/article-pdf/20/21/5496/2022082/5496.pdf by guest on 21 July 2024

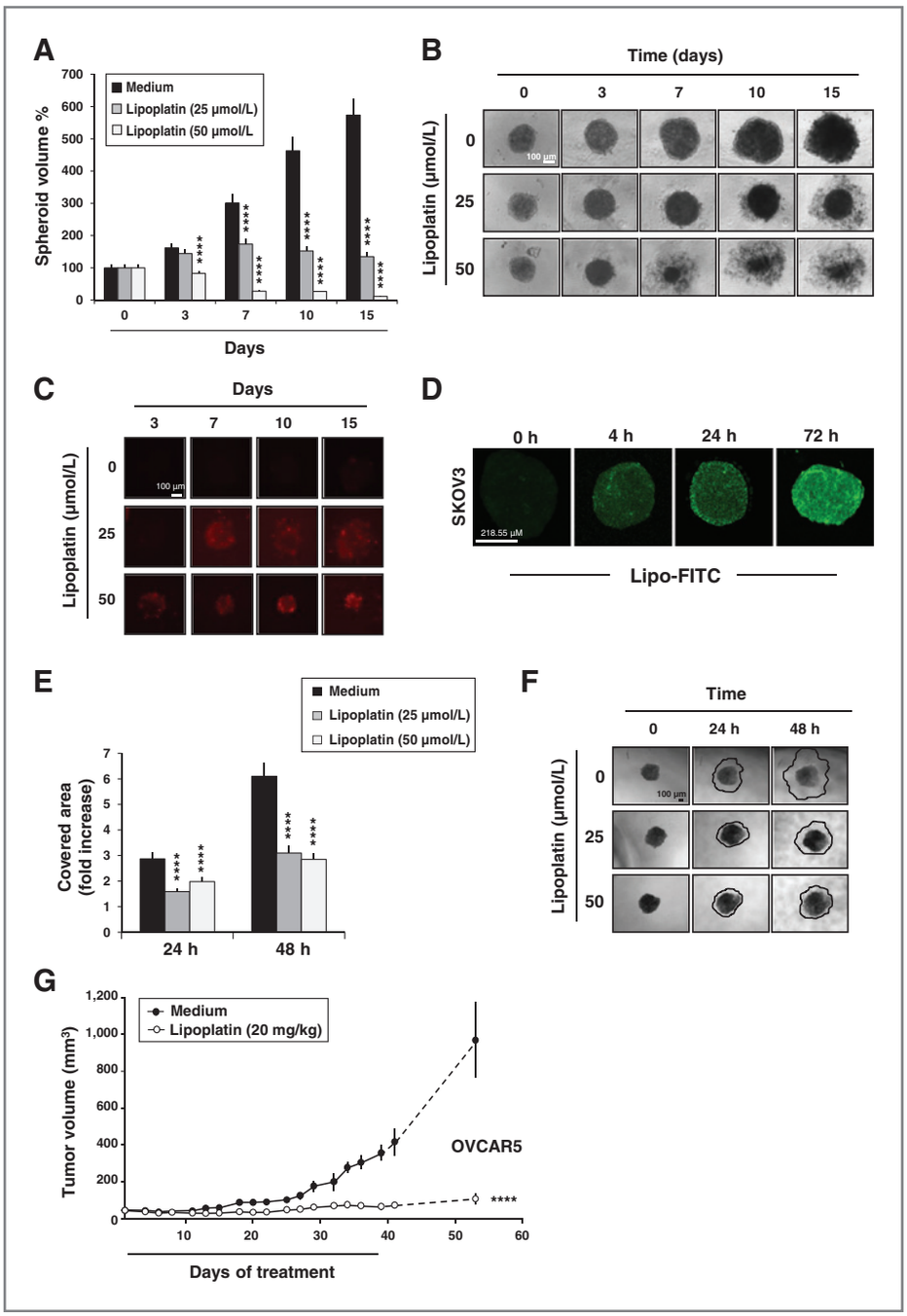

Figure 5. Lipoplatin inhibits spheroid growth, migration, and tumor xenograft. A, SKOV3 single preformed spheroids were cultured for 15 days in the absence or presence of lipoplatin (25, 50 μmol/L). Responses were evaluated by spheroid volume measurements at regular intervals. Values in the bar graph represent the mean ± SEM of 3 different experiments. ****, $P < 0.0001$ drug versus medium. B, representative phase contrast microphotographs showing volume decrease by lipoplatin treatment (original magnification, 4×). C, after lipoplatin treatment, spheroids were incubated with PI and then observed under fluorescence microscope. D, representative confocal images of FITC-labeled lipoplatin (Lipo-FITC) penetration into single SKOV3 spheroids. E and F, inhibition of migration/dissemination on matrix protein of SKOV3 spheroids by lipoplatin. SKOV3 single spheroids were placed on collagenase I–coated plates in the presence of lipoplatin (25, 50 μmol/L). E, histograms showing the migration rate of spheroids, evaluated as the area covered by migrating cells from spheroids and represented as fold increase respect to the area (pixel) covered at time = 0. ****, $P < 0.0001$ drug versus medium. Values in the bar graph represent the mean ± SEM of 3 different experiments. F, images were captured after 24 and 48 hours using an inverted microscope (phase contrast microphotographs; original magnification, 4×). G, *in vivo* anticancer activity of lipoplatin (OVCAR5 xenograft). Tumor volumes were measured in female athymic nude mice after intraperitoneal injection of medium, either drug-free- or containing 20 mg/kg lipoplatin, 3 times a week using a caliper. At day 39, treatment was suspended for 14 days (dashed lines). Each value represents the mean ± SEM of 8 animals per group. ****, $P < 0.0001$ lipoplatin versus control.

Downloaded from http://aacrjournals.org/clincancerres/article-pdf/20/21/5496/2022082/5496.pdf by guest on 21 July 2024

bulk of tumor cells and likely responsible for tumor relapse, the major clinical problem in cancer treatment.

Ovarian cancer cells are present in ascitic fluids either as single cells or as less or more compact macroaggregates, the latter contributing most to the spreading to secondary sites (28). In fact, these aggregates can travel through the ascitic fluid and attach to organs within the peritoneal cavity, a process that requires invasion of the mesothelial cell layer covering these organs (44). The 3D *in vitro* growth conditions (spheroids) recall several characteristics of ovarian cancer ascites cellular macroaggregates, including resistance to cisplatin, and represent a more reliable model than 2D cell cultures (45). Moreover, the present finding that lipoplatin inhibited the growth and the dissemination of cells from preformed spheroids is important. The positive relationship found between compact spheroid formation and invasive behavior (28) implies a preferential survival of an invasive subpopulation of ovarian cancer cells, as cells in spheroids are more resistant to several chemotherapeutics (11). Preventing/reducing ovarian cancer spheroids or reducing CSCs may represent a novel strategy to decrease metastases and to improve the efficacy of existing therapeutics. The data in this study support an additional property of lipoplatin, that of an antimetastasis drug.

Finally, while cisplatin used at the same concentration of lipoplatin (20 mg/kg) caused a severe toxicity in nude mice (46), lipoplatin inhibited tumor xenografts of OVCAR5 with minimal systemic toxicity, and even if the treatment was discontinued, no tumor progression was observed, suggesting that the schedule used was very effective. Moreover, lower doses of cisplatin (3 and 6 mg/kg) were either ineffective or effective but too toxic.

Monotherapy studies in lung cancer showing almost negligible (grade I) toxicity in human studies and a very high efficacy (38% partial response, 43% stable disease) as second-line treatment (47) establish lipoplatin as a very exciting drug of a high potential in the chemotherapy arsenal.

In conclusion, replacing cisplatin with lipoplatin in aggressive cisplatin-resistant patients with ovarian cancer would add the advantage of lower toxicities as already shown in randomized phase II and III studies in NSCLC (48–50). Adding the advantage of reducing the metastatic potential and the putative ovarian CSCs, and its synergistic activity with Abraxane and doxorubicin, lipoplatin in combination with Abraxane or doxorubicin should be compared with cisplatin + Abraxane/doxorubicin in a randomized clinical study against ovarian cancer.

Disclosure of Potential Conflicts of Interest

No potential conflicts of interest were disclosed.

Authors' Contributions

Conception and design: N. Casagrande, D. Aldinucci
Development of methodology: N. Casagrande,M. Celegato, C. Borghese, M. Mongiat
Analysis and interpretation of data (e.g., statistical analysis, biostatistics, computational analysis): N. Casagrande
Writing, review, and/or revision of the manuscript: N. Casagrande, A. Colombatti, D. Aldinucci
Study supervision: D. Aldinucci

Grant Support

This research was supported by Ministero della Salute, Ricerca Finalizzata FSN, I.R.C.C.S., Rome, Italy.

The costs of publication of this article were defrayed in part by the payment of page charges. This article must therefore be hereby marked *advertisement* in accordance with 18 U.S.C. Section 1734 solely to indicate this fact.

Received March 25, 2014; revised July 25, 2014; accepted August 10, 2014; published OnlineFirst September 17, 2014.

References

1. Coleman RL, Monk BJ, Sood AK, Herzog TJ. Latest research and treatment of advanced-stage epithelial ovarian cancer. Nat Rev Clin Oncol 2013;10:211–24.
2. Galluzzi L, Vitale I, Michels J, Brenner C, Szabadkai G, Harel-Bellan A, et al. Systems biology of cisplatin resistance: past, present and future. Cell Death Dis 2014;5:e1257.
3. Zalba S, Garrido MJ. Liposomes, a promising strategy for clinical application of platinum derivatives. Expert Opin Drug Deliv 2013;10: 829–44.
4. Liu D, He C, Wang AZ, Lin W. Application of liposomal technologies for delivery of platinum analogs in oncology. Int J Nanomedicine 2013;8:3309–19.
5. Seetharamu N, Kim E, Hochster H, Martin F, Muggia F. Phase II study of liposomal cisplatin (SPI-77) in platinum-sensitive recurrences of ovarian cancer. Anticancer Res 2010;30:541–5.
6. Stathopoulos GP, Boulikas T. Lipoplatin formulation review article. J Drug Deliv 2012;2012:581363.
7. Farhat FS, Temraz S, Kattan J, Ibrahim K, Bitar N, Haddad N, et al. A phase II study of lipoplatin (liposomal cisplatin)/vinorelbine combination in HER-2/neu-negative metastatic breast cancer. Clin Breast Cancer 2011;11:384–9.
8. Casagrande N, De Paoli M, Celegato M, Borghese C, Mongiat M, Colombatti A, et al. Preclinical evaluation of a new liposomal formulation of cisplatin, lipoplatin, to treat cisplatin-resistant cervical cancer. Gynecol Oncol 2013;131:744–52.
9. Boulikas T, Stathopoulos GP, Volakakis N, Vougiouka M. Systemic Lipoplatin infusion results in preferential tumor uptake in human studies. Anticancer Res 2005;25:3031–9.
10. Boulikas T. Molecular mechanisms of cisplatin and its liposomally encapsulated form, Lipoplatin. Lipoplatin as a chemotherapy and antiangiogenesis drug. Cancer Ther 2007;5:351–76.
11. Lee JM, Mhawech-Fauceglia P, Lee N, Parsanian LC, Lin YG, Gayther SA, et al. A three-dimensional microenvironment alters protein expression and chemosensitivity of epithelial ovarian cancer cells *in vitro*. Lab Invest 2013;93:528–42.
12. Chou TC, Talalay P. Quantitative analysis of dose-effect relationships: the combined effects of multiple drugs or enzyme inhibitors. Adv Enzyme Regul 1984;22:27–55.
13. Cattaruzza L, Fregona D, Mongiat M, Ronconi L, Fassina A, Colombatti A, et al. Antitumor activity of gold(III)-dithiocarbamato derivatives on prostate cancer cells and xenografts. Int J Cancer 2011;128:206–15.
14. Vinci M, Box C, Zimmermann M, Eccles SA. Tumor spheroid-based migration assays for evaluation of therapeutic agents. Methods Mol Biol 2013;986:253–66.
15. Shield K, Ackland ML, Ahmed N, Rice GE. Multicellular spheroids in ovarian cancer metastases: Biology and pathology. Gynecol Oncol 2009;113:143–8.
16. Bandekar A, Karve S, Chang MY, Mu Q, Rotolo J, Sofou S. Antitumor efficacy following the intracellular and interstitial release of liposomal doxorubicin. Biomaterials 2012;33:4345–52.

Downloaded from http://aacrjournals.org/clincancerres/article-pdf/20/21/5496/2022082/5496.pdf by guest on 21 July 2024

17. Dolznig H, Rupp C, Puri C, Haslinger C, Schweifer N, Wieser E, et al. Modeling colon adenocarcinomas *in vitro* a 3D co-culture system induces cancer-relevant pathways upon tumor cell and stromal fibroblast interaction. Am J Pathol 2011;179:487–501.
18. Mistry P, Kelland LR, Loh SY, Abel G, Murrer BA, Harrap KR. Comparison of cellular accumulation and cytotoxicity of cisplatin with that of tetraplatin and amminedibutyratodichloro(cyclohexylamine)platinum(IV) (JM221) in human ovarian carcinoma cell lines. Cancer Res 1992;52:6188–93.
19. Brozovic A, Ambriovic-Ristov A, Osmak M. The relationship between cisplatin-induced reactive oxygen species, glutathione, and BCL-2 and resistance to cisplatin. Crit Rev Toxicol 2010;40:347–59.
20. Mahmood DF, Abderrazak A, El HK, Simmet T, Rouis M. The thioredoxin system as a therapeutic target in human health and disease. Antioxid Redox Signal 2013;19:1266–303.
21. Pignata S, Scambia G, Ferrandina G, Savarese A, Sorio R, Breda E, et al. Carboplatin plus paclitaxel versus carboplatin plus pegylated liposomal doxorubicin as first-line treatment for patients with ovarian cancer: the MITO-2 randomized phase III trial. J Clin Oncol 2011;29:3628–35.
22. Pisano C, Cecere SC, Di NM, Cavaliere C, Tambaro R, Facchini G, et al. Clinical trials with pegylated liposomal Doxorubicin in the treatment of ovarian cancer. J Drug Deliv 2013;2013:898146.
23. Yared JA, Tkaczuk KH. Update on taxane development: new analogs and new formulations. Drug Des Devel Ther 2012;6:371–84.
24. Coleman RL, Brady WE, McMeekin DS, Rose PG, Soper JT, Lentz SS, et al. A phase II evaluation of nanoparticle, albumin-bound (nab) paclitaxel in the treatment of recurrent or persistent platinum-resistant ovarian, fallopian tube, or primary peritoneal cancer: a Gynecologic Oncology Group study. Gynecol Oncol 2011;122:111–5.
25. Glaysher S, Bolton LM, Johnson P, Atkey N, Dyson M, Torrance C, et al. Targeting EGFR and PI3K pathways in ovarian cancer. Br J Cancer 2013;109:1786–94.
26. Sugihara E, Saya H. Complexity of cancer stem cells. Int J Cancer 2013;132:1249–59.
27. Kryczek I, Liu S, Roh M, Vatan L, Szeliga W, Wei S, et al. Expression of aldehyde dehydrogenase and CD133 defines ovarian cancer stem cells. Int J Cancer 2012;130:29–39.
28. Sodek KL, Ringuette MJ, Brown TJ. Compact spheroid formation by ovarian cancer cells is associated with contractile behavior and an invasive phenotype. Int J Cancer 2009;124:2060–70.
29. Chahinian AP, Mandeli JP, Gluck H, Naim H, Teirstein AS, Holland JF. Effectiveness of cisplatin, paclitaxel, and suramin against human malignant mesothelioma xenografts in athymic nude mice. J Surg Oncol 1998;67:104–11.
30. Koch M, Krieger ML, Stolting D, Brenner N, Beier M, Jaehde U, et al. Overcoming chemotherapy resistance of ovarian cancer cells by liposomal cisplatin: molecular mechanisms unveiled by gene expression profiling. Biochem Pharmacol 2013;85:1077–90.
31. Stolting DP, Borrmann M, Koch M, Wiese M, Royer HD, Bendas G. How liposomal Cisplatin overcomes chemoresistance in ovarian tumour cells. Anticancer Res 2014;34:525–30.
32. Wu CC, Bratton SB. Regulation of the intrinsic apoptosis pathway by reactive oxygen species. Antioxid Redox Signal 2012;19:546–58.
33. Youle RJ, Strasser A. The BCL-2 protein family: opposing activities that mediate cell death. Nat Rev Mol Cell Biol 2008;9:47–59.
34. Liu Y, Li Y, Yu S, Zhao G. Recent advances in the development of thioredoxin reductase inhibitors as anticancer agents. Curr Drug Targets 2012;13:1432–44.
35. Powis G, Kirkpatrick DL. Thioredoxin signaling as a target for cancer therapy. Curr Opin Pharmacol 2007;7:392–7.
36. Witte AB, Anestal K, Jerremalm E, Ehrsson H, Arner ES. Inhibition of thioredoxin reductase but not of glutathione reductase by the major classes of alkylating and platinum-containing anticancer compounds. Free Radic Biol Med 2005;39:696–703.
37. Tillmanns TD, Lowe MP, Walker MS, Stepanski EJ, Schwartzberg LS. Phase II clinical trial of bevacizumab with albumin-bound paclitaxel in patients with recurrent, platinum-resistant primary epithelial ovarian or primary peritoneal carcinoma. Gynecol Oncol 2013;128:221–8.
38. Noske A, Schwabe M, Weichert W, Darb-Esfahani S, Buckendahl AC, Sehouli J, et al. An intracellular targeted antibody detects EGFR as an independent prognostic factor in ovarian carcinomas. BMC Cancer 2011;11:294–11.
39. Vergote IB, Jimeno A, Joly F, Katsaros D, Coens C, Despierre E, et al. Randomized phase III study of erlotinib versus observation in patients with no evidence of disease progression after first-line platin-based chemotherapy for ovarian carcinoma: a European Organisation for Research and Treatment of Cancer-Gynaecological Cancer Group, and Gynecologic Cancer Intergroup study. J Clin Oncol 2014;32:320–6.
40. Nakayama K, Nakayama N, Katagiri H, Miyazaki K. Mechanisms of ovarian cancer metastasis: biochemical pathways. Int J Mol Sci 2012;13:11705–17.
41. Liebscher CA, Prinzler J, Sinn BV, Budczies J, Denkert C, Noske A, et al. Aldehyde dehydrogenase 1/epidermal growth factor receptor coexpression is characteristic of a highly aggressive, poor-prognosis subgroup of high-grade serous ovarian carcinoma. Hum Pathol 2013;44:1465–71.
42. Landen CN Jr, Goodman B, Katre AA, Steg AD, Nick AM, Stone RL, et al. Targeting aldehyde dehydrogenase cancer stem cells in ovarian cancer. Mol Cancer Ther 2010;9:3186–99.
43. Skubitz AP, Taras EP, Boylan KL, Waldron NN, Oh S, Panoskaltsis-Mortari A, et al. Targeting CD133 in an *in vivo* ovarian cancer model reduces ovarian cancer progression. Gynecol Oncol 2013;130:579–87.
44. Iwanicki MP, Davidowitz RA, Ng MR, Besser A, Muranen T, Merritt M, et al. Ovarian cancer spheroids use myosin-generated force to clear the mesothelium. Cancer Discov 2011;1:144–57.
45. Kwon MJ, Shin YK. Regulation of ovarian cancer stem cells or tumor-initiating cells. Int J Mol Sci 2013;14:6624–48.
46. Chahinian AP, Norton L, Holland JF, Szrajer L, Hart RD. Experimental and clinical activity of mitomycin C and cis-diamminedichloroplatinum in malignant mesothelioma. Cancer Res 1984;44:1688–92.
47. Stathopoulos GP, Stathopoulos J, Dimitroulis J. Two consecutive days of treatment with liposomal cisplatin in non-small cell lung cancer. Oncol Lett 2012;4:1013–6.
48. Stathopoulos GP, Antoniou D, Dimitroulis J, Stathopoulos J, Marosis K, Michalopoulou P. Comparison of liposomal cisplatin versus cisplatin in non-squamous cell non-small-cell lung cancer. Cancer Chemother Pharmacol 2011;68:945–50.
49. Mylonakis N, Athanasiou A, Ziras N, Angel J, Rapti A, Lampaki S, et al. Phase II study of liposomal cisplatin (Lipoplatin) plus gemcitabine versus cisplatin plus gemcitabine as first line treatment in inoperable (stage IIIB/IV) non-small cell lung cancer. Lung Cancer 2010;68:240–7.
50. Stathopoulos GP, Antoniou D, Dimitroulis J, Michalopoulou P, Bastas A, Marosis K, et al. Liposomal cisplatin combined with paclitaxel versus cisplatin and paclitaxel in non-small-cell lung cancer: a randomized phase III multicenter trial. Ann Oncol 2010;21:2227–32.

Downloaded from http://aacrjournals.org/clincancerres/article-pdf/20/21/5496/2022082/5496.pdf by guest on 21 July 2024